ISSN 1560-0904, Polymer Science, Ser. B, 2014, Vol. 56, No. 6, pp. 736–743. © Pleiades Publishing, Ltd., 2014.



# Poly(styrene-methyl methacrylate) Microcapsules Prepared by Ultrasonically Initiated Miniemulsion Polymerization Phase Separation Method[1]

**S. W. Guo[a,b], G. X. Wang[a], G. H. Geng[a], and F. L. Han[a]**

[a] *College of Materials Science and Engineering, Beifang University of Nationalities, Yinchuan 750021, China*

[b] *State Key Laboratory of Polymer Materials Engineering, Polymer Research Institute, Sichuan University, Chengdu 610065, China*

*e-mail: feidehai@163.com*

Received July 24, 2014;
Revised Manuscript Received September 29, 2014

**Abstract**—Ultrasonically initiated miniemulsion polymerization phase separation was employed to prepare poly(styrene-methyl methacrylate) (P(St–*co*–MMA)) microcapsules. The results of a thermal analysis revealed that it was difficult to form a microcapsule structure from neat styrene (St). However, MMA shows improved interface conditions due to its higher hydrophilicity than St. Therefore, it was easier to form hollow structures because the polymer microcapsules had a lower interface free energy per unit area. The results of dynamic light scattering (DLS), transmission electron microscopy (TEM) and atomic force microscopy (AFM) showed that P(St–*co*–MMA) microcapsules were uniform in size (about 100 nm in diameter and 20–25 nm in shell thickness).

**DOI:** 10.1134/S1560090415010030

## INTRODUCTION

In recent years, polymer microcapsules have drawn broad attention in academic research and practical applications owing to their unique structures and functions [1–3]. They could be used as chemical reactors with well defined properties, drug delivery vehicles and protective shells in the fields of organic synthesis, biochemistry and material science [4–6]. There are many approaches to obtain polymer microcapsules [7–11].

Ultrasound is a kind of mechanical vibration waves in a frequency range of $2 \times 10^4$–$10^7$ Hz [12]. When it transmits through a liquid medium, ultrasonic cavitation occurs, which generates a very extreme local environment, i.e. extremely high local temperature and pressure, as well as great heating and cooling rate [13, 14]. A polymerization reaction can be realized without initiator at room temperature under an ultrasonic field. Furthermore, ultrasonically initiated polymerization always exhibits a high reaction rate.

The essence of polymerization phase separation method (PPSM) is the liquid core technology. Polymer microcapsules have narrow size distribution and controllable shell thickness with PPSM. Polymerization phase separation method mainly includes two steps: phase separation owing to polymerization and evaporation of solvent. That is, with carrying on of polymerization, the polymer chain is propagating continuously. The compatibility with dispersed phase gradually deteriorates. And the polymer chain will transfer to the interface of two phases. Hollow structure then occurs. In this paper, sonochemistry and miniemulsion polymerization phase separation method was combined to prepare P(St–*co*–MMA) microcapsules. And sonochemistry was further developed in the field of new-style materials preparation. This is a simple, clean and environment-friendly technology.

## EXPERIMENTAL

### *Materials*

Methyl methacrylate (MMA) was purchased as analytical grade from Tianjin Bodi chemical Co., Ltd., China. It was washed with 10% aqueous sodium hydroxide and water to remove the inhibitor and dried over anhydrous sodium sulfate, then was distilled under reduced pressure prior to use. The sealed purified sample was stored at 4°C until required. Styrene (St) was purchased as analytical grade from Chengdu Kelong chemical reagent factory, China. Its purification process was same as MMA.

Hexadecane (HD), isooctane (IOT) and sodium dodecyl sulfate (SDS) were also purchased as analytical grade from Chengdu Kelong chemical reagent factory. They were used as received.

[1] The article is published in the original.

### *Apparatus*

The equipment employed in this research is a Model VCF–1500 ultrasonic generator (Sonics and Materials) with a frequency of 20 kHz. The titanium probe has a diameter of 25 mm. Ultrasonic irradiation was carried out with the probe of the ultrasonic horn immersed directly in the reaction system. During the polymerization, thermostated water was circulated to maintain the temperature constant, and $N_2$ purging rate kept constant.

### *Preparation of P(St–co–MMA) Microcapsules through Ultrasonically Initiated Miniemulsion Polymerization Phase Separation*

MMA, St, HD and IOT were mixed under magnetic stirrer. The mixture was then added into the aqueous solution of SDS and buffer. They were placed into the reaction vessel, deoxygenated by bubbling with oxygen-free $N_2$ for 5 min. Then the ultrasound generator was switched on and the miniemulsion polymerization was initiated by ultrasound irradiation. During the polymerization process, the $N_2$ flow rate was kept at 50 mL/min, the cooling water was circulated to maintain at a temperature of 20°C, and the power output of ultrasound was 900 W. The acoustic intensity generated at the tip of the horn and adsorbed by the solution was measured by a special instrument (YP0511F acoustometer, Hangzhou Success Ultrasonic Equipment Co., Ltd, China) to be 16.5 W/cm$^2$. After a certain reaction time, ultrasonic irradiation was stopped. P(St–*co*–MMA) microcapsules were obtained. A part of the prepared polymer emulsion was poured into ice-cold ethanol to coagulate and demulsify, then the precipitated material was filtered, washed, dried under vacuum condition, and tested with FTIR and weighed to ascertain the conversion gravimetrically in the usual way. The remaining emulsion was determined with DLS, TEM and AFM directly.

### *Characterization*

Samples were removed at various times throughout the ultrasonic irradiation and the monomer conversion was determined gravimetrically. A portion $v$, in units of ml, of emulsion was dried at 50°C until a constant weight $w$, in units of g, was obtained. The monomer conversion is defined as follows:

$$\text{Conversion}(\%) = \frac{w(V/v) - m_1 - m_2}{m_M} \times 100\%, \quad (1)$$

where $m_1$, $m_2$ and $m_M$ are the charged weights of SDS, buffer, and monomer, respectively, and V is the total volume of emulsion.

Dynamic light scattering experiments were performed in 10 mm diameter round quartz precision light scattering cells at an angle of 90° and at 298 K. The apparatus employed was a BI–200SM spectrogoniometer (Brookhaven, USA) equipped with an Innova 304 $Ar^+$ laser operating at a wavelength of 532 nm and BI-9000AT digital correlator.

Fourier transform infrared analysis was performed on a Nicolet 560 spectrometer with scanning over the range of 500–4000 cm$^{-1}$.

The morphologies and structures of P(St–*co*–MMA) microcapsules were determined by transmission electron microscopy (TEM) on a JEM 100 CX instrument (JEOL Co., Japan). One drop of the suspension was diluted into water and placed on a 400-mesh carbon-coated copper grid and dried in air before observation.

AFM testing was performed on a Nanoscope Multimode Explore (USA). For AFM imaging, two or three drops of the concentrated dispersion were cast on freshly cleaned mica plates and allowed to air dry. AFM images were obtained in the ''tapping'' mode. Maximum horizontal scanning range: 125 × 125 μm.

## RESULTS AND DISCUSSION

### *FTIR Analysis*

The FTIR spectrum of PMMA, PSt and P(St–*co*–MMA) microcapsules prepared through ultrasonically initiated miniemulsion polymerization phase separation are illustrated in Fig. 1 (curves *1*–*3*, respectively). In Fig. 1 (curve *1*), 1731 cm$^{-1}$ corresponds to the stretching vibration of C=O. 1390 cm$^{-1}$ corresponds to the symmetrical deformation vibration. Furthermore, 2999, 2953 and 2845 cm$^{-1}$ are the typical absorption peaks corresponding to the stretching vibration of $-CH_3$ and $-CH_2$. In Fig. 1 (curve *2*), 2921 and 2849 cm$^{-1}$ also correspond to the stretching vibration of $-CH_2$. 3025 and 3059 cm$^{-1}$ correspond to the stretching vibration of unsaturated hydrocarbon group on benzene ring. 1452, 1493 and 1601 cm$^{-1}$ are the typical peaks of benzene skeleton vibration. 698 and 754 cm$^{-1}$ correspond to the out-plane bending vibration of unsaturated hydrocarbon group on benzene ring. Moreover, 1745, 1803, 1871 and 1943 cm$^{-1}$ correspond to the overtones and combinations of out-plane deformation vibration of C–H on single substitution benzene ring [15]. Obviously, there are both PMMA's and PSt's spectral characteristics in Fig. 1 (curve *3*).

### *DLS Analysis*

Dynamic light scattering (DLS) is the most important technique for directly detecting cluster populations in solution [16]. It uses photon correlation spectroscopy (PCS) and consists of analyzing the time fluctuations of the light scattered by optically anisotropic particles subjected to Brownian motion in a solvent of a given viscosity. The monochromatic laser light scattered by a solution at a given angle is analyzed in terms of the temporal field autocorrelation function

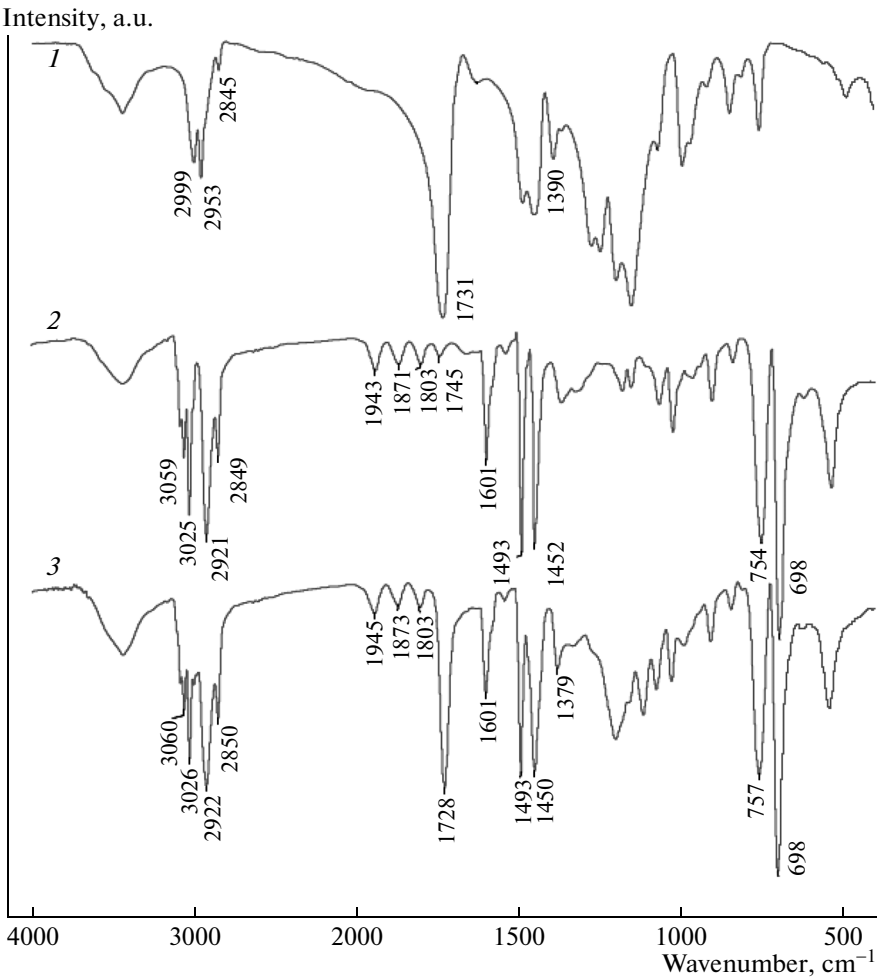


**Fig. 1.** FTIR spectra of (*1*) PMMA, (*2*) PS and (*3*) P(St–*co*–MMA) microcapsules prepared through ultrasonically initiated miniemulsion polymerization.

$C(\tau)$ sampled over a wide range of times $\tau$. Considering this motion in terms of translational and rotational diffusion, the dimensions of the particles can be determined as a drastic change in the time-intensity correlation function. By contrast with imaging techniques, DLS does not need the drying of the dispersion and the measurements are performed faster.

When the ultrasonically initiated miniemulsion polymerization phase separation was finished, the emulsion was diluted to an appropriate concentration with deionized water. The particle size and distribution of P(St–*co*–MMA) microcapsules are presented in Fig. 2. The average size of polymer microcapsules is 110 nm. And the polydispersity index (PDI) is 0.164. These results show that P(St–*co*–MMA) microcapsules are monodisperse. Furthermore, correlation function is a statistical method to study fluctuation phenomenon of PCS. As it is seen from Fig. 2, the measured baseline and the calculated baseline are highly coincident. That is to say, the optical purification of samples is in good quality. It shows a better fitting and the testing results are believable.

### *TEM Analysis*

When ultrasonically initiated miniemulsion polymerization with single monomer-St was employed, a few microcapsules can be found (shown in Fig. 3). On the contrary, most of them are the solid PSt latex particles. In addition, the size distribution of polymer microcapsules is broad, i.e., the polydispersity index is large. However, when MMA was introduced as comonomer, the above case was improved obviously (shown in Fig. 4). The number of polymer microcapsules was significantly increased in the ultimate product. And the size of these microcapsules is greater than 100 nm, their wall thickness is 20–25 nm. They are nearly monodisperse, i.e., the size distribution is very narrow. The TEM's results are consistent with the DLS's tests very much.

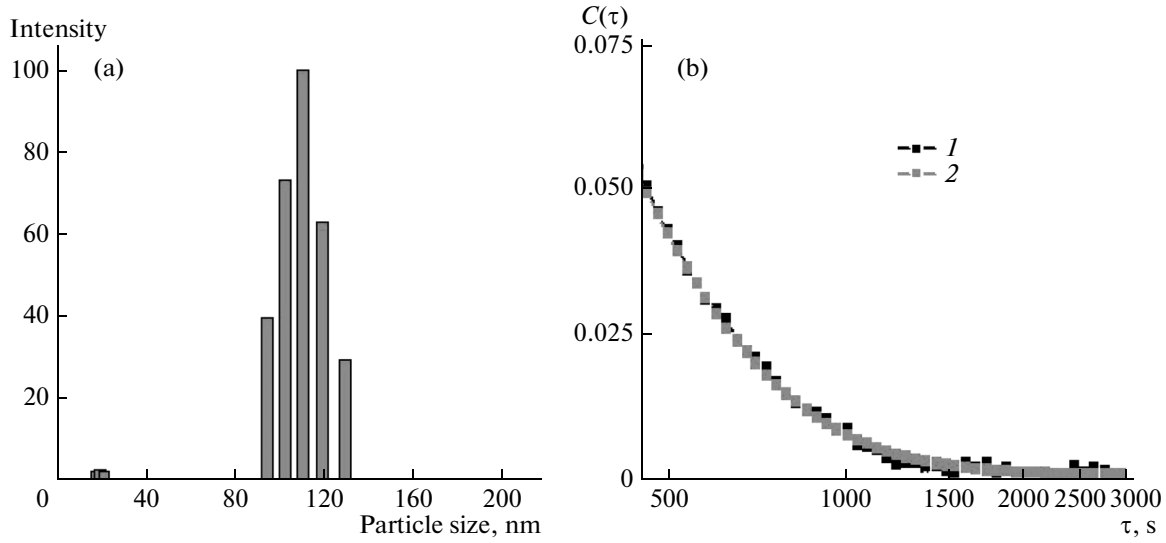


**Fig. 2.** (a) Size and (b) distribution of P(St–*co*–MMA) microcapsules: (*1*) measured baseline, (*2*) calculated baseline.

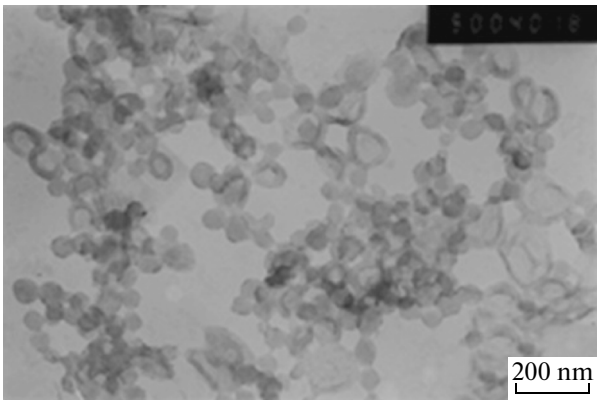


**Fig. 3.** TEM photograph of polymer microcapsules prepared through ultrasonically initiated miniemulsion polymerization with pure St.

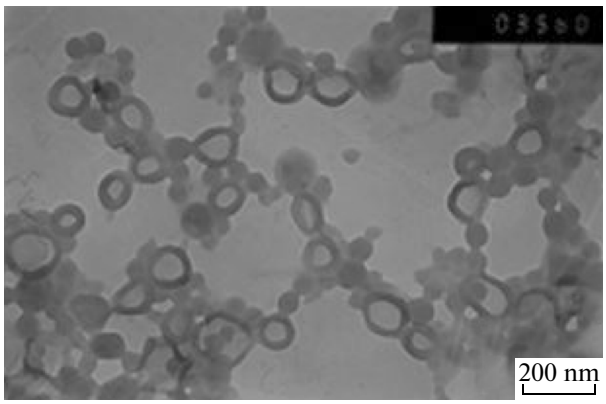


**Fig. 4.** TEM photograph of polymer microcapsules prepared through ultrasonically initiated miniemulsion polymerization with St and MMA.

The reason is that MMA has a better hydrophilicity than that of St. St is just a typical kind of hydrophobic monomer. When the polymerization reaction was started, the interfacial tension between PSt and continuous phase became larger. That is to say, the spreading coefficient of PSt in oil droplets is small. Therefore, it is difficult to transfer to the interface between two phases from IOT. With carrying on of the polymerization reaction, the viscosity of oil phase increased due to PSt which couldn't diffuse immediately. It further hindered the diffusion from the inner to the outer of the follow-up new polymer. So, the ultimate product would certain to be the solid PSt latex particles, which was determined by both thermodynamic and kinetic factors. The hollow structure could not be obtained. However, when adding MMA comonomer, the interfacial tension between polymer and continuous phase was improved. And the copolymer's spreading coefficient became lager. It could transfer to the interface easier. The follow-up copolymer wouldn't be blocked, either. That is, a lot of channels were provided for the diffusion of copolymer. Therefore, it is reasonable that a large number of P(St–*co*–MMA) microcapsules (hollow structure) were eventually formed in the product.

### *AFM Analysis*

After the film-forming of P(St–*co*–MMA) microcapsules on freshly cleaned mica plates, AFM was performed in the ''tapping'' mode (Fig. 5). The images were obtained by detecting the difference between the phase angle of signal source which drove the vibration of micro-cantilever probe and the phase angle of actual vibration of micro-cantilever probe (phase shift). From AFM topological image (Fig. 5a), the

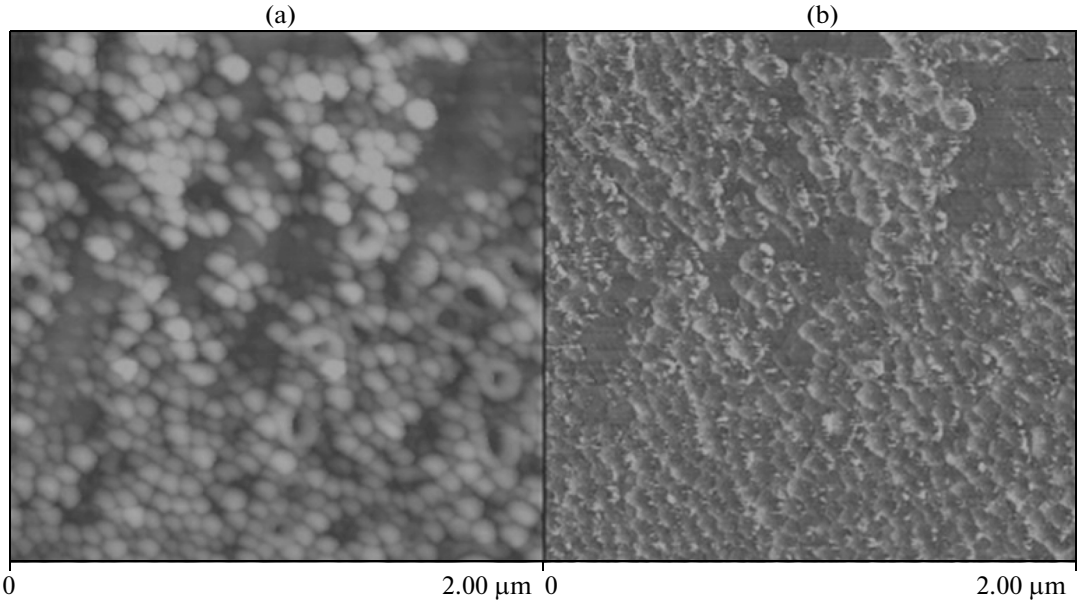


**Fig. 5.** AFM (a) topological image and (b) phase image of P(St–*co*–MMA) microcapsules prepared through ultrasonically initiated miniemulsion.

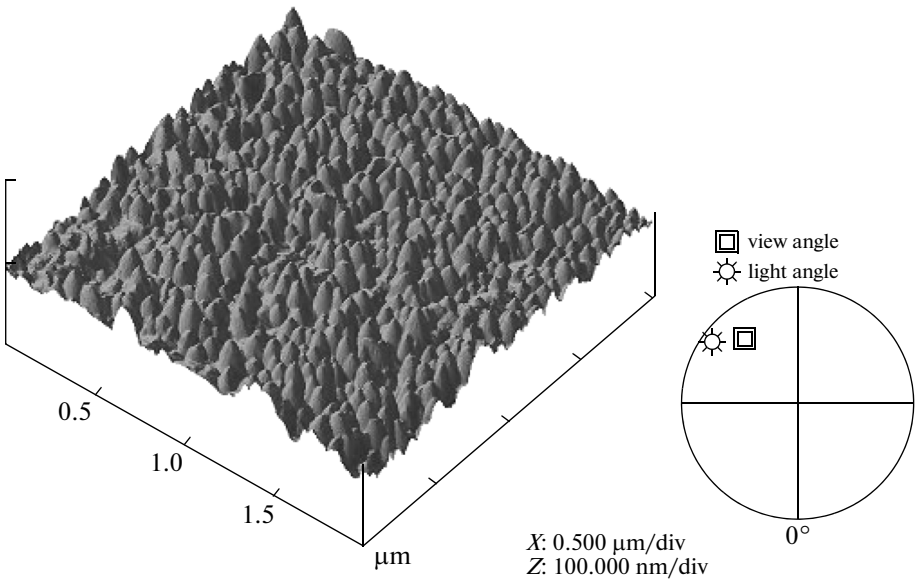


**Fig. 6.** AFM surface plot of P(St–*co*–MMA) microcapsules prepared through ultrasonically initiated miniemulsion polymerization.

monodisperse polymer microcapsules with homogeneous size prepared through ultrasonically initiated miniemulsion polymerization phase separation could be found. It should be noted that some of these microcapsules have "hemisphere" or "bowl" structure, which resulting from the collapse in the process of sampling or testing.

AFM measurement has a tip broadening effect in the horizontal direction. The smaller the target size, the more obvious the broadening effect. This would lead to a deviation of testing results. However, there is no the above effect in the vertical direction. So the measurement results are very accurate. That is to say, the particle size is denoted by three-dimensional height. Obviously, the size of P(St–*co*–MMA) microcapsules is 100 nm. And they have good uniformity (Fig. 6). These results are consistent with those of DLS and TEM.

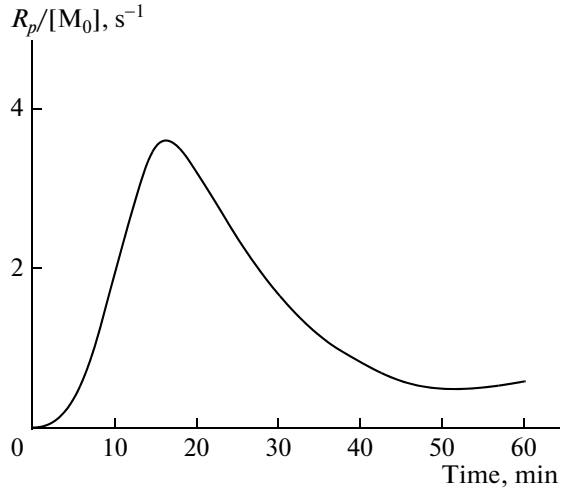


**Fig. 7.** Total polymerization rate vs. time curve for ultrasonically initiated miniemulsion polymerization of St and MMA ($v_{St}/v_{MMA} = 4/1$, $v_{monomer}/v_{water} = 1/30$, power intensity: 16.5 W/cm$^2$).

### *Thermodynamic Analysis*

In 1970s, Torza and Mason systematically studied the three-phase interfacial system. And their theory has been widely recognized [17]. According to the theory, there are three phases in our study, i.e., P(St–*co*–MMA) (phase 1), IOT (phase 2) and water (phase 3). The formation process of polymer microcapsules could be estimated by calculating the spreading coefficient $S$ of different phase.

$$S_i = \sigma_{jk} - (\sigma_{ij} + \sigma_{ik}), \quad (2)$$

$$\sigma_{ij} = \sigma_i + \sigma_j - 2(\sigma_i^d \sigma_j^d)^{1/2} - 2(\sigma_i^h \sigma_j^h)^{1/2}, \quad (3)$$

where $\sigma$ is the interfacial tension between two phases, $\sigma^d$ is the dispersion force of interfacial tension, $\sigma^h$ is the hydrogen bond force of interfacial tension. $\sigma$, $\sigma^d$ and $\sigma^h$ of water are known. If the interfacial tension between any phase and water is known, $\sigma^d$ and $\sigma^h$ of this phase could be calculated. And then, the interfacial between it and the third phase could be also obtained.

The interfacial tension and its forces at 20°C of different phase were listed in Table according to the literature [18] and our calculating.

According to Eq. (2), the interfacial tension between different two phases could be calculated: $\sigma_{12} = 33.4$ mN/m, $\sigma_{23} = 50$ mN/m, $\sigma_{13} = 40$ mN/m.

$\sigma$, $\sigma^d$, and $\sigma^h$ of water, IOT, PSt and PMMA (mN/m)

| | Water | IOT | PSt | PMMA |
|---|---|---|---|---|
| $\sigma$ | 72.8 | 20.55 | 42 | 40.2 |
| $\sigma^d$ | 21.8 | 20.13 | 41.4 | 35.9 |
| $\sigma^h$ | 51 | 0.42 | 0.6 | 4.3 |

The interfacial tension of P(St–*co*–MMA) was calculated by linear summation of two components according to molar fraction.

Furthermore, according to Eq. (1), the spreading coefficient of P(St–*co*–MMA), IOT and water is $S_1 = -23.4$ mN/m, $S_2 = -43.4$ mN/m and $S_3 = -56.6$ mN/m, respectively. In the interfacial equilibrium theory of Torza and Mason, when $S_1 < 0$, $S_2 < 0$ and $S_3 > 0$, phase 2 could be completely gulped by phase 1. And then, polymer microcapsules could be obtained. When $S_1 < 0$, $S_2 < 0$ and $S_3 < 0$, phase 2 could be partially gulped by phase 1. And polymer microcapsules and "bowl" structure microcapsules would coexist in the system. And when $S_1 < 0$, $S_2 > 0$ and $S_3 < 0$, polymer microcapsules would not be prepared. As noted above, only small quantities of P(St–*co*–MMA) microcapsules can be obtained when adopting single monomer St. However, the interfacial condition would be improved between different phases when introducing relatively hydrophilic monomer MMA. At this point, it was easier to form hollow structure because polymer microcapsules had a lower interface free energy per unit area. And the encapsulation driving force of P(St–*co*–MMA) at the periphery of IOT was increased.

### *Kinetic Analysis*

The mechanism of miniemulsion polymerization is very different from that of conventional emulsion polymerization and microemulsion polymerization [19, 20]. Therein, the strong hydrophobic costabilizer is an important feature of miniemulsion polymerization. The covering layer which was formed by surfactant on the surface of droplet would adjust the droplet size and prevent the coalescence among them. Ostwald ripening effect could be effectively inhibited by the osmotic pressure generated from the costabilizer. And the stable monomer miniemulsion on kinetics would be obtained. The monomer droplet size in miniemulsion is ca. 100 nm. These monomer droplets have strong ability to absorb radicals in continuous phase due to their enormous surface area. On one hand, micellar nucleation can be avoided by controlling the concentration of emulsifier (less than its critical micelle concentration). On the other hand, the oligomeric radicals in aqueous phase would be scavenged by monomer droplets with enormous surface area before reaching their critical soluble length. So the nucleation in aqueous phase can be neglected. That is to say, monomer droplets become the main polymerization nucleation sites.

Just as shown in Fig. 7, the first stage of polymerization is the nucleation process of latex particles. The maximum polymerization rate occurs when the conversion rate reaches 30%. It indicated the end of the first stage polymerization reaction. Since then, the polymerization rate began to decline into the decreasing speed stage-the second stage of polymerization. In

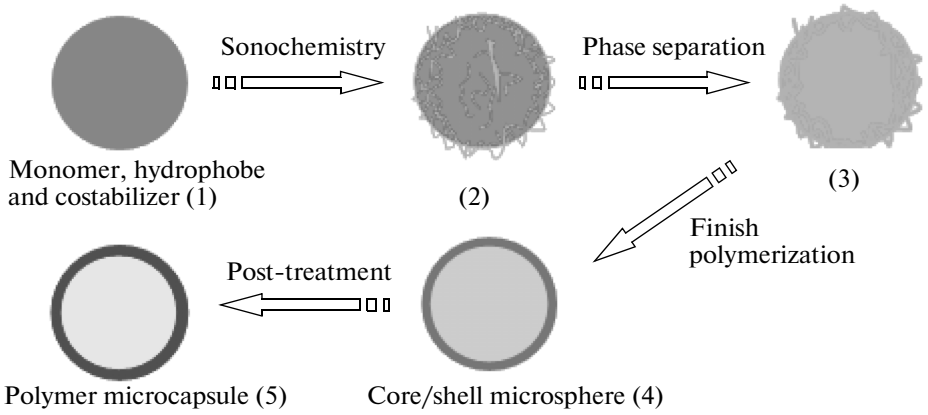


**Scheme 1.**

miniemulsion polymerization, there is no constant speed stage because the new latex particles are always being generated. So, in the first stage, the polymerization rate is gradually increased. And then it will decrease when the conversion rate reaches a platform. The reason is that the consumed monomer can not be supplied from the monomer house any more.

In fact, there is no classic "three steps" feature in any ultrasonically initiated polymerization reaction. That is, there is no apparent constant speed stage. The reason lies in monomer droplets have similar specific surface area with solubilization micelles under ultrasonic field. Therefore, they both are the main polymerization nucleation sites. The number of active sites is not constant in the process of polymerization. And the nucleation always exists throughout the whole reaction.

### *The Mechanism of Ultrasonically Initiated Miniemulsion Polymerization Phase Separation*

State 1 is a droplet composed of HD, IOT, MMA and St (see below). HD is a common costabilizer in miniemulsion polymerization. It was used to prevent the coalescence resulting from Ostwald ripening effect among these droplets. IOT is just used as a kind of soft template (liquid core). P(St–*co*–MMA) gradually emerged in droplet when ultrasonically initiated miniemulsion polymerization was employed. The compatibility of the copolymer with the droplet is worse than that of the monomer. It would certain to transfer to the interface between two phases by the driving force of interfacial tension. So the concentration of P(St–*co*–MMA) on the droplet surface is higher than that in the droplet center (state 2). With the carrying on of the polymerization, the monomer would be used up. And all copolymers would transfer to the periphery of the droplets to form a dense shell (state 3, 4). At this point, there is only liquid core-IOT in the polymer microcapsules. After the polymerization, the true P(St–*co*–MMA) microcapsules can be obtained by drying the product in a vacuum to remove IOT (state 5). Just as in the analysis of thermodynamics, the control of each phase's spreading coefficient is very important in the process of ultrasonically initiated miniemulsion polymerization phase separation. That is to say, the follow-up new polymer must transfer to the surface of the droplets in a short time. Otherwise, the ultimate product would certain to be a solid polymer latex particle rather than a true polymer microcapsule.

## CONCLUSIONS

Polymer microcapsules were obtained by applying sonochemistry technology in the soft-template method. It proved the universality of sonochemistry method in preparation of this kind of new-style materials. Ultrasonically initiated miniemulsion polymerization phase separation was employed to prepare P(St–*co*–MMA) microcapsules. And the formation mechanism was investigated. Thermodynamic analysis indicated it was difficult to form the hollow structure when only a single monomer-St was used. However, the interfacial condition could be improved by introducing another monomer-MMA with relatively higher hydrophilicity. The interface free energy per unit area of forming polymer microcapsules became smaller. And the driving force of forming a polymer shell in the periphery of IOT was increased. So it was easier to get P(St–*co*–MMA) microcapsules. Kinetic analysis showed that the monomer conversion reached 80% in 60 min. And there was no constant speed stage in ultrasonically initiated miniemulsion polymerization. It was just a feature of ultrasonically initiated polymerization reaction. DLS, TEM and AFM results showed that P(St–*co*–MMA) microcapsules had a uniform size of about 100 nm. Their wall thickness was ~20–25 nm. And the polydispersity index was small.

## ACKNOWLEDGMENTS

This work was supported by the 2013 "Western Light" Talent Culture Project of Chinese Academy of Sciences, the Natural Science Foundation of Ningxia, project no. NZ11141 and the Key Laboratory of Powder Material and Special Ceramics, project no. 201101.

## REFERENCES

1. G. Sukhorukov, A. Fery, and H. Mohwald, Prog. Polym. Sci. **30**, 885 (2005).
2. B. Huang, F. Bai, X. L. Yang, and W. Q. Huang, Chin. J. Polym. Sci. **28**, 277 (2010).
3. F. Caruso, Adv. Mater. **13**, 11 (2001).
4. I. Gill and A. Ballesteros, J. Am. Chem. Soc. **120**, 8587 (1998).
5. Y. Y. Wang, T. Q. Liu, and W. W. Xu, Chem. Res. Chin. Univ. **29**, 607 (2013).
6. G. Cevc, J. Controlled Release **160**, 135 (2012).
7. V. V. Istratov, V. T. Tarasyuk, V. A. Vasnev, and N. A. Borisova, Polym. Sci., Ser. B **55**, 218 (2013).
8. X. Y. Liu, M. Jiang, S. L. Yang, M. Q. Chen, D. Y. Chen, C. Yang, K. Wu, Angew. Chem., Int. Ed. **41**, 2951 (2002).
9. H. Lv, Q. Lin, K. Zhang, K. Yu, T. J. Yao, X. H. Zhang, J. H. Zhang, and B. Yang, Langmuir **24**,13736 (2008).
10. P. W. Chen, R. M. Erb, and A. R. Studart, Langmuir 28, 144 (2012).
11. T. J. Yao, Q. Lin, K. Zhang, D. F. Zhao, H. Lv, J. H. Zhang, and B. Yang, J. Colloid Interface Sci. **315**, 434 (2007).
12. L. Reynold, Philos. Mag. **34**, 94 (1917).
13. K. S. Suslick, Science **247**, 1439 (1990).
14. K. S. Suslick, D. A. Harnmerton, and R. E. Cline, J. Am. Chem. Soc. **108**, 5641 (1986).
15. Y. C. Ning, *Structural Identification of Organic Spectroscopy* (Science Press, Beijing, 2010).
16. G. Min, E. Sheina, G. D. Patterson, M. A. Bevan, and D. C. Prieve, Colloids Surf., A **202**, 9 (2002).
17. S. Torza and S. G. Mason, J. Colloid Interface Sci. **33**, 67 (1970).
18. D. W. VanKrevelen, *Properties of Polymers* (Science Press, Beijing, 1981).
19. Y. T. Choi, M. S. El-Aasser, E. D. Sudol, and J. W. Vanderhoff, J. Polym. Sci., Part A: Polym. Chem. **23**, 2973 (1985).
20. N. Bechthold and K. Landfester, Macromolecules **33**, 4682 (2000).